ARTICLE

Peptide-Grafted Nontoxic Cyclodextrins and Nanoparticles against Bacteriophage Infections

Łukasz Richter,* Corey Alfred Stevens, Paulo Jacob Silva, Laura Roset Julià, Carla Malinverni, Lixia Wei, Marcin Łoś, and Francesco Stellacci*

Read Online

ACCESS | Metrics & More | Article Recommendations | Supporting Information

ABSTRACT: One of the biggest threats for bacteria-based bioreactors in the biotechnology industry is infections caused by bacterial viruses called bacteriophages. More than 70% of companies admitted to encountering this problem. Despite phage infections being such a dangerous and widespread risk, to date, there are no effective methods to avoid them. Here we present a peptide-grafted compounds that irreversibly deactivate bacteriophages and remain safe for bacteria and mammalian cells. The active compounds consist of a core (cyclodextrin or gold nanoparticle) coated with a hydrophobic chain terminated with a peptide selective for bacteriophages. Such peptides were selected via a phage display technique. This approach enables irreversible deactivation of the wide range of T-like phages (including the most dangerous in phage infections, phage T1) at 37 °C in 1 h. We show that our compounds can be used directly inside the environment of the bioreactor, but they are also a safe additive to stocks of antibiotics and expression inducers (such as isopropyl β-D-1-thiogalactopyranoside, i.e., IPTG) that cannot be autoclaved and are a common source of phage infections.

KEYWORDS: bacteriophages, peptides, nanoparticles, cyclodextrins, phage infections, biotechnology industry, bacteria
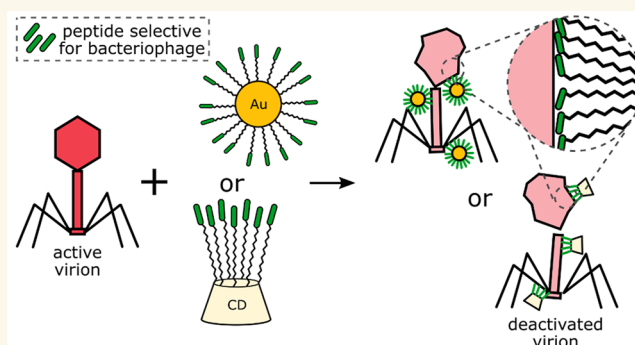
INTRODUCTION

One of the most important aspects of biotechnology and food industries is bacteria-based processes. We learned to exploit the natural abilities of bacteria to mass-produce a wide range of products crucial in our daily life, such as ethanol, dairy products, antibiotics, probiotics, enzymes, organic acids, and even fuels and solvents.[1] One of the most dangerous and common risks for all bacterial processes is contamination with bacterial viruses, i.e., bacteriophages. More than 70% of biotechnological companies have admitted to encountering this problem, and 1−10% of product batches are considered to be lost due to phage infections.[1]

Phage contaminations are extremely difficult to prevent due to two main reasons. First, phages are the most abundant organisms on Earth. There are estimated to be around 10^{31} phages on our planet, and they are a component of any ecosystem containing bacteria.[2] Therefore, there are multiple routes of phage contamination, such as dry products, process air, water, and even working staff. Second, even a few virions have the ability to contaminate a whole production batch in

just a few hours and produce up to 10^{13} pfu/mL.[3] During infection, tens or even hundreds of progeny phages are released from every single infected bacterium.

To date, the most common approach against phage contaminations is to autoclave the whole bioreactor content before aseptic inoculation of the process. However, this approach does not provide absolute protection. Phages can survive elevated temperature, high pressure, pasteurization, drying, and even vacuum.[4] Moreover, autoclaving cannot be applied to stocks of antibiotics and expression inducers (such as IPTG), as this would inactivate them. Consequently, it is believed that often these solutions of additives cause phage contaminations. After infection, typically the whole production
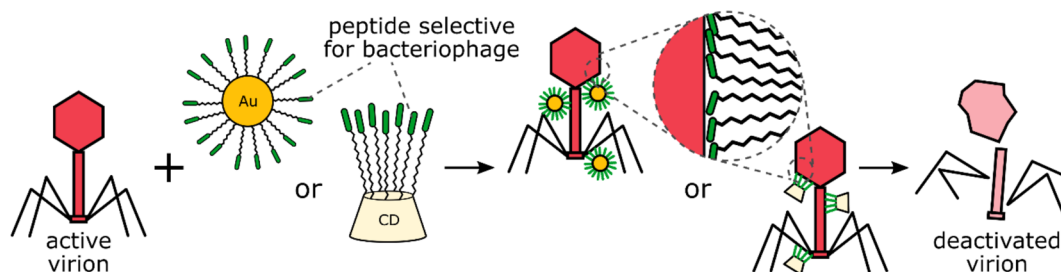
Figure 1. Schematic drawing of the activity of the prepared antiphage compounds. Cyclodextrins or nanoparticles first attach to phages due to interaction with selective peptides and then virions are deactivated by irreversible local distortions.
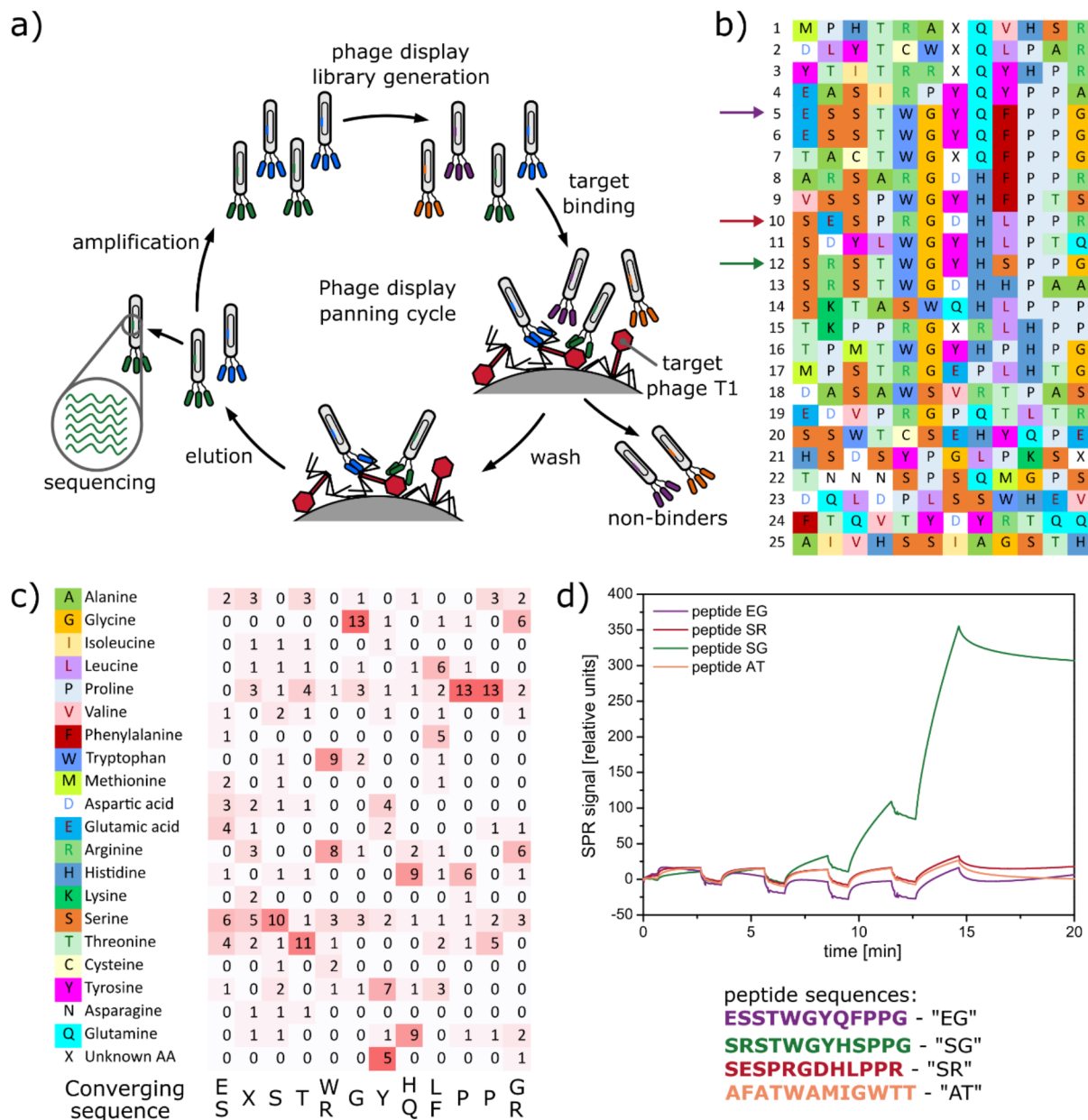

Figure 2. (a) Schematic presentation of phage display cycles used for identification of peptides selective for bacteriophages T1. (b) Sequences of 25 peptides collected after the last cycle of phage display. Arrows indicate the peptide most similar to the converging sequence and therefore selected for surface plasmon resonance (SPR) test. (c) Converging sequence method applied to identify selective peptides. For every position in the peptide, the most common amino acid was selected. (d) SPR measurement of the interaction between various peptides and phages T1. Consecutive waves in every curve correspond to increasing concentrations of phages in the applied mobile phase.
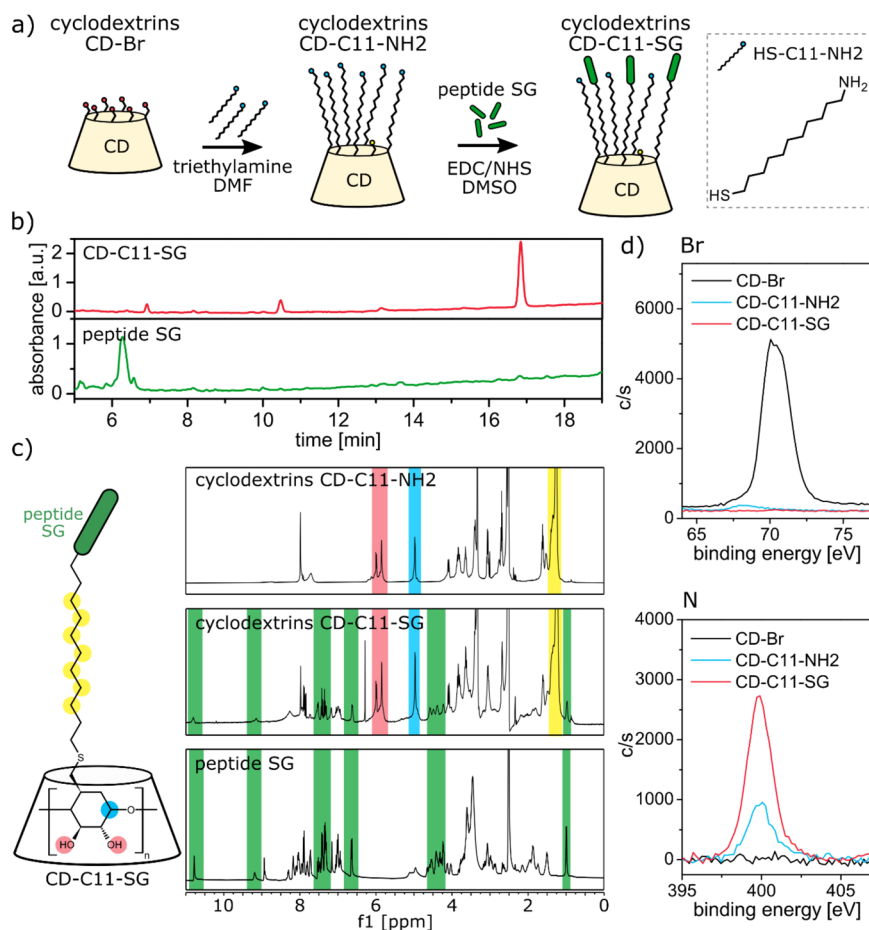
Figure 3. Synthesis and characterization of the prepared peptide-modified cyclodextrins. (a) Scheme of the synthesis of the cyclodextrins. The addition of hydrophobic linkers to the cyclodextrin core was then followed by modification with peptides. (b) High-performance liquid chromatography (HPLC) characterization of obtained CD-C11-SG cyclodextrins. (c) ^{1}H NMR of cyclodextrins and peptide SG, showing the desired composition of the final product: cyclodextrin core, hydrophobic linkers, and peptides. (d) X-ray photoelectron spectroscopy (XPS) analysis of bromine (Br) and nitrogen (N). Absence of Br signal in CD-C11-NH2 and CD-C11-SG shows effective addition of hydrophobic linker. An increasing amount of nitrogen in CD-C11-NH2 and then CD-C11-SG indicates effective addition of hydrophobic linker followed by successful modification with peptide SG.

line has to be closed and cleaned thoroughly, which is a long and costly operation.[5] Instead, the ideal approach should allow to deactivate bacteriophages before the outbreak and to create a protective environment for bacteria directly inside the environment of the bioreactor.

Over the last few decades next to standard decontamination methods, such as thermal treatment, filtration, ethylene oxide,[6,7] and UV radiation,[8−12] many novel solutions were proposed to avoid phage infections, such as metal (silver,[13−17] iron−nickel)[18] or metal oxide (copper oxide,[15,17,19] titanium dioxide),[20,21] nanoparticles, proteins,[22−24] biocides,[9,25] phage-resistant strains,[26] and methods based on the rotation of bacterial strains.[8] However, all of these are limited by issues related to large volumes, high cost, narrow specificity, high cytotoxicity, low efficiency, regulatory problems, or only preventive effects. In our recent work, we showed virucidal nanoparticles effective against phage infections and safe for bacteria.[27] However, due to their initial binding mechanism relying solely on electrostatic interactions, long incubation times (up to 24 h), and elevated temperature (50 °C) were required.

Here, we present a next-generation approach to designing antiphage protective solutions: peptide-based virucidal com-pounds irreversibly deactivating a wide range of T-like phages (including the most dangerous in industrial phage infections, phage T1)[5] at 37 °C in just 1 h. Our compounds consist of a core (cyclodextrin or gold nanoparticle) coated with a hydrophobic chain ended with a peptide selective for bacteriophages (Figure 1). They are harmless for bacteria and safe for mammalian cells. They can be used directly inside the environment of the bioreactor or as a safe additive to stocks of antibiotics and expression inducers (such as IPTG). The presented approach is inspired by previous work done in our group that focused on glycan-[28] or sulfonate-based[29,30] antivirals against mammalian enveloped viruses. It should be highlighted that we are showing that such an antiviral approach can be used against water-borne viruses and with a peptide as a targeting compound. Additionally, our approach works on nonenveloped viruses.

RESULTS AND DISCUSSION

Phage Display. Our goal was to achieve effective and irreversible deactivation of phages while remaining nontoxic for bacteria and eukaryotic cells. In the case of eukaryotic viruses, this goal can be achieved using sulfate-coated nanoparticles[29] and cyclodextrins[30] against HSPG-dependent
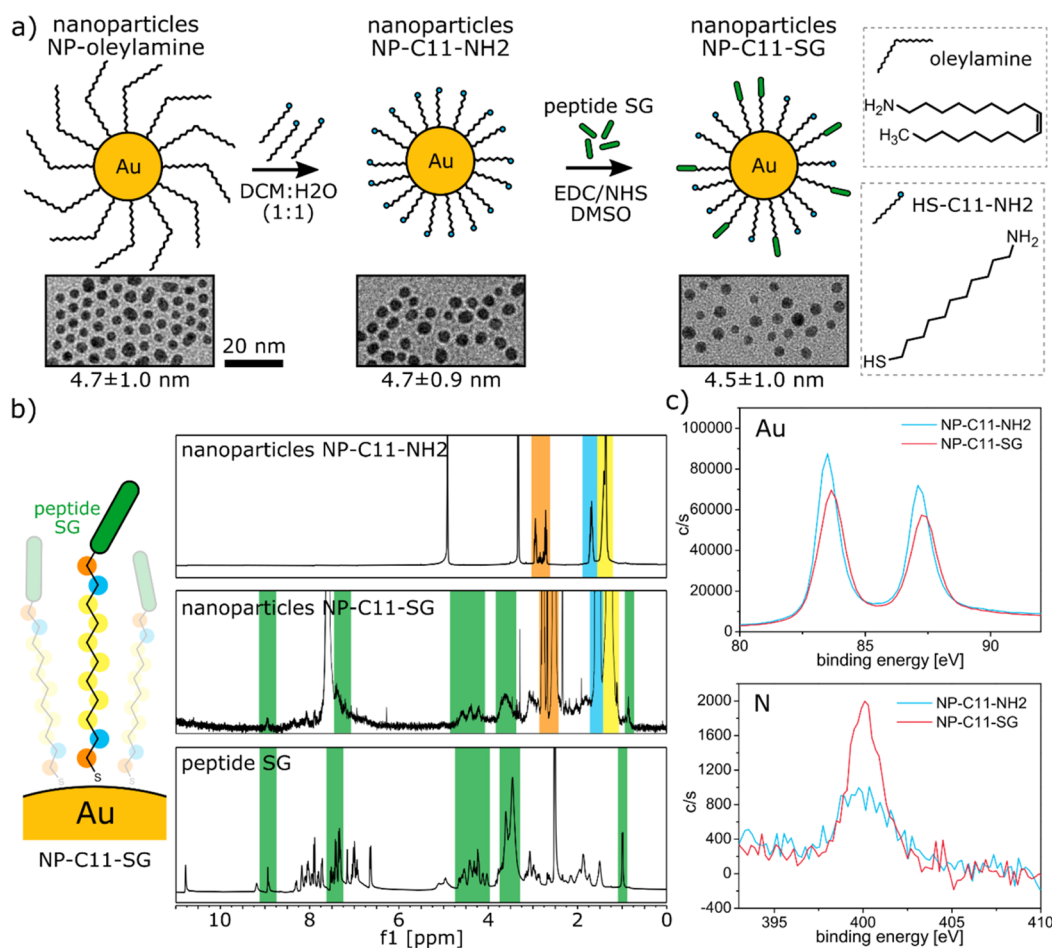
Figure 4. Synthesis and characterization of the prepared peptide-modified nanoparticles. (a) Scheme of synthesis of the nanoparticles, composed of ligand exchange followed by attachment of peptides. For each step, the size distribution and representative TEM are presented. The gold core of the nanoparticles was not disturbed throughout the whole synthesis and their size remained the same. (b) ^{1}H NMR of etched nanoparticles and peptide SG, showing the final ligand composition: hydrophobic linkers modified with peptides. (c) X-ray photoelectron spectroscopy (XPS) analysis of gold (Au) and nitrogen (N). An increase of the amount of nitrogen and a slight decrease of the amount of gold in the case of CD-C11-SG indicates effective modification with peptide SG.

viruses and sialic acid-coated cyclodextrins[28] against influenza virus. Unfortunately, due to the complex, multistep infection mechanism of bacteriophages, typically including transmembrane proteins of bacteria, this approach is ineffective.[31] Here we developed another approach targeted our antiviral compounds to bacteriophages resulting in selective and strong phage interaction.

To circumvent such complexity, we used phage display, a biological combinatorial technique, to identify short peptides selective for the bacteriophages known to cause industrial infections. Since the starting point of phage display is a randomized library of millions of peptide sequences, this approach vastly expands the possibilities of high-throughput screening. In this technique, the target bacteriophage T1 was exposed to 2 million random peptides that were 7 or 12 amino acids long. The most strongly interacting peptides were selected through iterative biopanning cycles (Figure 2). We decided to use whole virions instead of the selected part of the bacteriophage, such as a single purified protein. This way, the entire bacteriophage was exposed to peptides during the selection step, and we had the best chance to find peptides providing the highest interaction.

After three rounds of biopanning, we sequenced 25 randomly selected phages collected after the elution step (Figure 2b). We applied the method of the converging sequence, which means that for every position in the peptide sequence we selected the most common amino acid (Figure 2c). Then, we picked among sequenced peptides the three most similar to the converging sequence (peptides "EG", "SG", and "SR"). As a next step, surface plasmon resonance (SPR) was used to compare the interaction between T1 phages and three selected peptides (Figure 2d). In this technique, we first immobilized the tested peptides in microfluidic channels, and then a solution of T1 phages was run through those channels. The SPR signal was used to quantify phage attachment to the peptides. The randomly generated peptide "AT" was used as a negative control. SPR analysis showed that the peptide with sequence SRSTWGYHSPPG (peptide SG) interacted the strongest with phages T1 and therefore was used in the following preparation of antiphage compounds.

Peptide-Grafted Cyclodextrins. After identifying a peptide selective against bacteriophage T1, the next step was to prepare peptide-grafted cyclodextrins. First, we modified β-cyclodextrins brominated only on the primary face with 11-amino-1-undecanethiol ligands to obtain molecule CD-C11-
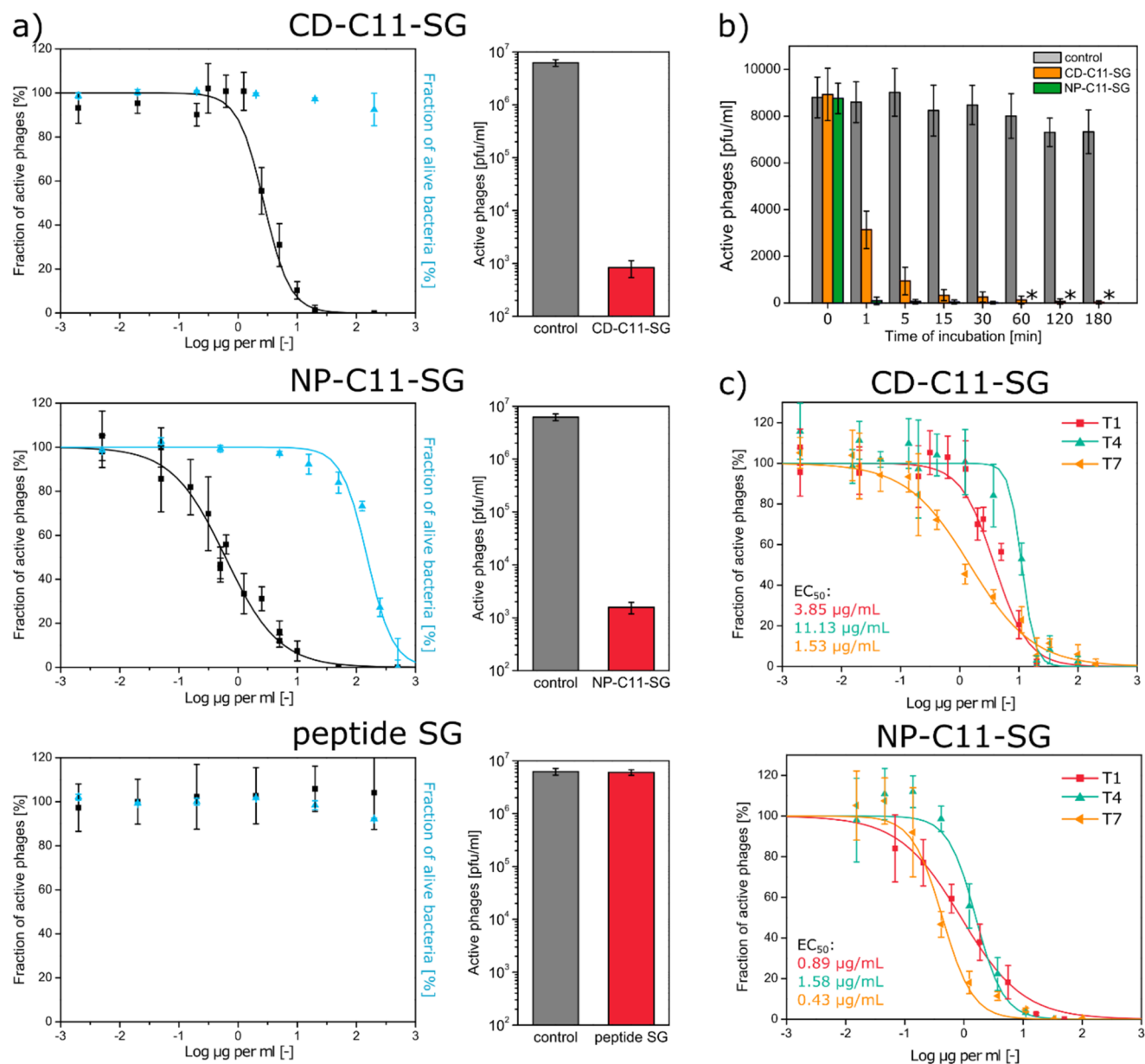
Figure 5. Antiviral properties of antiphage compounds. (a) dose−response phage infectivity curves (left) and virucidal assays (right) of cyclodextrins CD-C11-SG, nanoparticles NP-C11-SG, and peptide SG. (b) CD-C11-SG and NP-C11-SG inhibition of viral infectivity against phage T1 versus time. *, no phages were detected. (c) Dose−response phage infectivity curves of CD-C11-SG and NP-C11-SG against various types of T-like phages.

NH2 (Figure 3a). In this step, we obtained on average 6 ligands per cyclodextrin molecule, which was confirmed with the analysis of the ^{1}H NMR (Figure S1). Next, the peptide SG was attached to CD-C11-NH2 cyclodextrins via EDC/NHS reaction in DMSO. To avoid creating chains of peptides, we used peptides with the N-terminus protected with the fluorenylmethoxycarbonyl (Fmoc) protecting group (Figure S2). We characterized each obtained compound with ^{1}H NMR (Figure 3c) and proved that the final cyclodextrin CD-C11-SG is composed of cyclodextrin core, hydrophobic chains, and peptides. Correct attachment of ligands via thiol groups to the cyclodextrin cores was confirmed with ^{1}H NMR analysis of the signal coming from the aliphatic hydrogens (Figure S3). [1]H diffusion-ordered spectroscopy nuclear magnetic resonance

(^{1}H DOSY NMR) showed that for both CD-C11-NH2 and CD-C11-SG all signals share the same diffusion coefficient and thus come from various parts of the same molecule (Figure S4).

As a next characterization step, we performed an X-ray photoelectron spectroscopy (XPS) analysis of all three types of cyclodextrins (Figure 3d). The bromine signal, strongly visible in sample CD-Br, disappeared in samples CD-C11-NH2 and CD-C11-SG, confirming the successful attachment of 11-amino-1-undecanethiol (HS-C11-NH2) ligands to the cyclodextrins. Moreover, the nitrogen signal appeared in sample CD-C11-NH2, confirming attachment of HS-C11-NH2, and it then increased in the sample CD-C11-SG, which confirms effective attachment of peptides (16.4% of their overall mass is
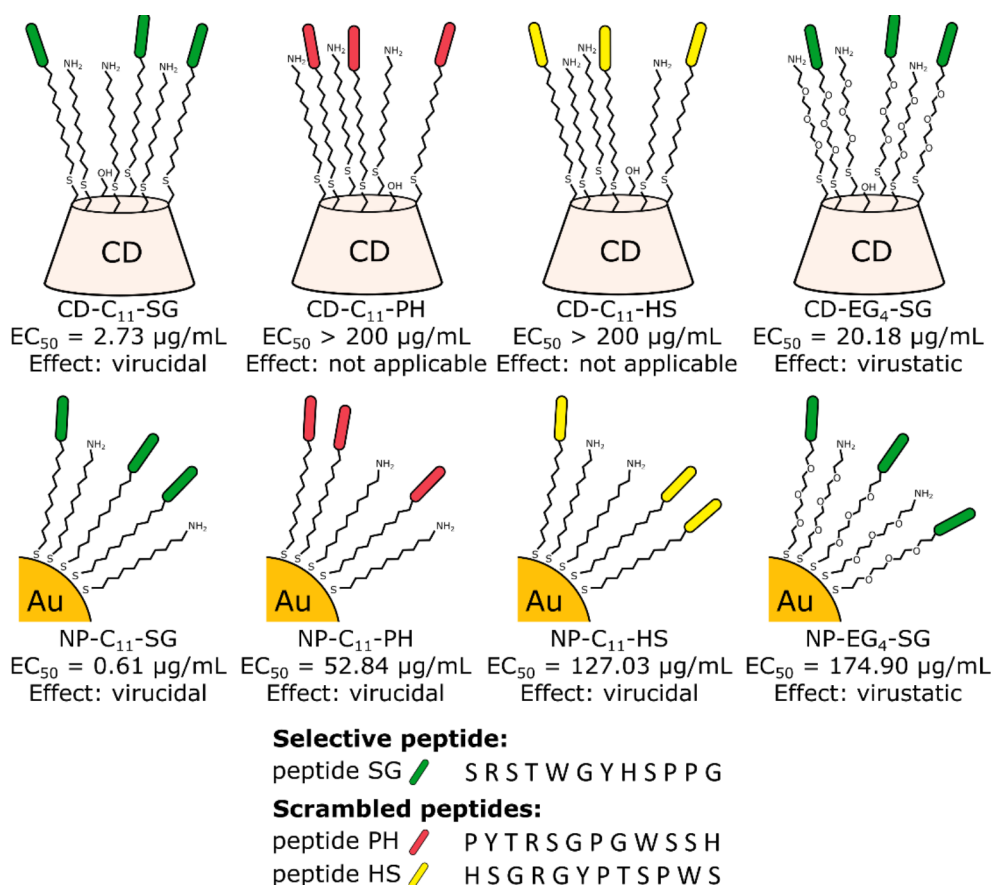
Figure 6. Summary of a library of all prepared nanoparticles and cyclodextrins. To evaluate the importance of the peptide sequence, we prepared compounds with scrambled versions of peptides (CD-C11-PH, CD-C11-HS, NP-C11-PH, and CP-C11-HS). To investigate the necessity of hydrophobic linkers, we synthesized compounds with hydrophobic linkers (CD-EG4-SG and NP-EG4-SG).

nitrogen). The high complexity of peptide signal in ^{1}H NMR did not allow for quantitative analysis, so we used XPS to investigate the number of peptides per cyclodextrin. Quantitative analysis of XPS signals not only confirmed an average number of 6 ligands per CD-C11-NH2 cyclodextrin but also showed that there are, on average, 3 peptides per CD-C11-SG cyclodextrin (Table S1). The purity of the molecules was also analyzed with high-performance liquid chromatography (HPLC). As presented in Figure 3b, one main fraction is visible (CD-C11-SG with 3 grafted peptides). Two other smaller fractions are most likely cyclodextrins with one and two peptides grafted, respectively.

Peptide-Grafted Nanoparticles. The second type of prepared antiphage compounds were peptide-coated nanoparticles. Their preparation consisted of three steps and started from the synthesis of oleylamine-coated nanoparticles (Figure 4a). Then, ligand exchange was performed to create nanoparticles NP-C11-NH2. The last step was EDC/NHS reaction to attach peptides to aminated ligands on the nanoparticles. Also, in this case, we used peptides with N-terminus protected with the Fmoc group. TEM images showed that the synthesis did not alter the size of the nanoparticles, which remained in a range of 4.5 ± 1.0 nm (Figure 4a). ^{1}H NMR analysis of the etched nanoparticles[32] confirmed that ligands on the final nanoparticles are composed of hydrophobic chains modified with peptides (Figure 4b). To further study the effectiveness of peptide grafting, we performed an XPS analysis (Figure 4c). Both the increase of the nitrogen signal and the decrease of the

gold signal confirmed the successful attachment of the peptides. Quantitative analysis of the XPS signals showed that every nanoparticle was functionalized on average with 33 peptides (Table S2).

Antiviral and Antibacterial Properties. To test the inhibitory activity of our compounds against phage T1, we performed a dose–response assay. First, phages were incubated at 37 °C for 3 h with either the nanoparticles or the cyclodextrins. Then, the number of active phages was analyzed using the plaque count method. As a control, we used the peptide SG alone. As presented in Figure 5a, both the peptide-grafted nanoparticles and the cyclodextrins showed good antiphage activity, with effective concentrations deactivating 50% of bacteriophages (EC$_{50}$) of 0.61 and 3.85 μg/mL, respectively. The blue points on these plots show dose–response against bacteria *Escherichia coli* BL21 proving that antiphage compounds are safe for bacteria. In each case, EC$_{50}$ against *E. coli* was at least 2 orders of magnitude higher than EC$_{50}$ against phages.

To further investigate whether the antiphage effect is irreversible (virucidal) or only reversible (virustatic), we performed virucidal assays. In this assay, after an initial incubation of phages with antiphage compounds, the sample was diluted and, in this way, virustatic (i.e., reversible) effects were eliminated. Thus, in virucidal assays only an irreversible effect was detected. As presented on bar plots in Figure 5a, both cyclodextrins CD-C11-SG and nanoparticles NP-C11-SG were found to be virucidal.

Discussion on the Mechanism of Action. The approach presented here to create our antiphage compounds was inspired by previous work done in our group on virucidal antiviral compounds (based on both nanoparticles and cyclodextrins).[28−30] In all cases the antiviral mechanism was the same: an initial interaction with the virus-driven by a binding moiety (sulfonic acid in case of HSPG-depended viruses, glycans in case of influenza viruses) followed by a secondary interaction with the hydrophobic aliphatic chains causing local destabilization of the virus structure. Our antiphage compounds have the same structural design and should have a similar mechanism of action. In this case, the initial interaction with selective peptide is followed by interaction with hydrophobic linker causing irreversible destabilization of the virion.

To further investigate the deactivating mechanism, we performed antiviral tests at various time points (Figure 5b). We showed that strong effects were visible after just 1 h. A similar time scale was reported in the case of other aforementioned antiviral compounds,[29] supporting the hypothesis of a common deactivation mechanism. It is important to state that virustatic effects based on binding are fast; it is the complexity of the virucidal mechanism that introduces processes on the scale of minutes.

To test the importance of the hydrophobic linkers, we prepared cyclodextrins and nanoparticles with hydrophilic (poly(ethylene glycol)) chains, decorated with selective peptide SG (Figure 6). All of the prepared compounds were characterized (Figures S11−S13), and for each of them dose−response assay and virucidal tests were performed (Table 1,

Table 1. Comparison of Antiviral, Antibacterial, and Cytotoxic Properties of All Prepared Compounds[a]

compound	EC$_{50}$ (T1) [µg/mL]	mechanism	CC$_{50}$ (*E. coli*) [µg/mL]	SI	CC$_{50}$ (Vero) [µg/mL]
NPs-C11-SG	0.61	virucidal	152.17	249.75	>500
NPs-C11-HS	127.02	virucidal	435.90	3.43	>500
NPs-C11-PH	52.84	virucidal	>500	>9.47	>500
NPs-EG4-SG	174.88	virustatic	>500	>2.86	>500
CD-C11-SG	2.73	virucidal	>200	>73.26	>200
CD-C11-HS	>200	not applicable	>200	n.a.	>200
CD-C11-PH	>200	not applicable	>200	n.a.	>200
CD-EG4-SG	20.18	virustatic	>200	>9.90	>200
peptide SG	>200	not applicable	>200	n.a.	>200
peptide HS	>200	not applicable	>200	n.a.	>200
peptide PH	>200	not applicable	>200	n.a.	>200

[a]EC$_{50}$ is effective concentration deactivating 50% of bacteriophages. CC$_{50}$ is a cytotoxic concentration killing 50% of bacterial or mammalian cells. Selective index (SI) is a ratio between CC$_{50}$ (*E. coli*) and EC$_{50}$ (T1).

Figure S14). Compounds with hydrophilic (poly(ethylene glycol)) linkers turned out to be only virustatic, confirming that hydrophobic interaction is crucial for virucidal action.

As a next step, we evaluated the selectivity of our compounds and showed that both compounds were effective against three types of T phages: T1, T4, and T7 (Figure 5c). This result was expected, since phages T1, T4, and T7 share a common head−tail structure, and many of their structural proteins have a similar structure.[33−35] Most likely, the peptide SG targets common motifs present in all three types of phages. Another possible explanation can be that peptide SG is a so-called "sticky peptide", i.e., it interacts nonspecifically with a broad range of targets.[35,36] To evaluate this possibility, we prepared a broader library of antiphage compounds, including compounds with scrambled peptides.

Library of Antiphage Compounds. To evaluate the effectiveness of our design of antiphage compounds, we created a set of control cyclodextrins and nanoparticles. First, to evaluate the properties of the selective peptide SG, we prepared and characterized compounds decorated with scrambled peptides called PH and HS (Figures 6 and S5−S8) If the hypothesis about peptide SG being a "sticky peptide" were correct, then the order of the amino acids should not matter much, and the scrambled peptides should have similar efficacy.

For every antiphage compound, we performed dose−response assays and virucidal tests. The compounds with scrambled peptides were much less effective against phages than compounds with peptide SG (Table 1, Figures S9 and S10), which indicates the importance of the selective sequence of the peptide. It also supports the explanation that peptide SG targets structural motifs common to T1, T4, and T7 phages.

Finally, we checked the influence of all prepared compounds on bacterial and eukaryotic cells, by performing (1) toxicity assay against bacteria *E. coli* BL21 and (2) cytotoxicity MTS assay against eukaryotic Vero cells (Table 1, Figure S15). In the first test, we let bacteria grow in the presence of various concentrations of antiphage compounds. In the latter, we first incubated cells with various concentrations of antiphage compounds for 24 h and then the viability of cells was evaluated by MTS assay. We proved that all compounds were safe for bacteria (SI > 200) and eukaryotic cells (EC$_{50}$ > 200 µg/mL).

Application Test on Infected Bacteria-Based Bioreactors. We tested the best performing antiphage compounds, CD-C11-SG and NP-C11-SG, in real-life application to protect bacteria directly inside the environment of a bioreactor. First, we added 50 µg/mL nanoparticles or cyclodextrins to a solution containing 500 pfu/mL T1 bacteriophages. This step was to mimic the addition of the antiphage compounds to an infected liquid inside a bioreactor. Such solution was incubated at 37 °C for 3 h, and then an inoculum of bacteria *E. coli* was added to it. Bacterial growth was observed via optical density measurement (OD$_{600}$). As control samples, we used noncontaminated solution (positive control) and solution contaminated with phages but without any antiphage additives (negative control) (Figure 7a). The addition of antiphage compounds resulted in successful deactivation of T1 bacteriophages and normal growth of protected bacteria (Figure 7b). Then, we evaluated the influence of the concentration of antiphage compounds and the time of incubation (Figure 7c). We showed that 1 h of incubation with 50 µg/mL CD-C11-SG cyclodextrins is enough for effective protection. Alternatively, 1 h of incubation with 50 µg/mL NP-C11-SG or 3 h of incubation with 5 µg/mL NP-C11-SG also induces a protective effect.

Application Test of Infected Stocks of Kanamycin and IPTG. To test possible applications even further, we prepared stocks of antibiotic kanamycin and expression inducer isopropyl β-D-1-thiogalactopyranoside (ITPG) in-

stocks (Figure 8a). After 24 h of growth at 37 °C, the optical density at wavelength 600 nm was measured (Figure 8b). In the case of samples 2 and 6 (prepared with contaminated
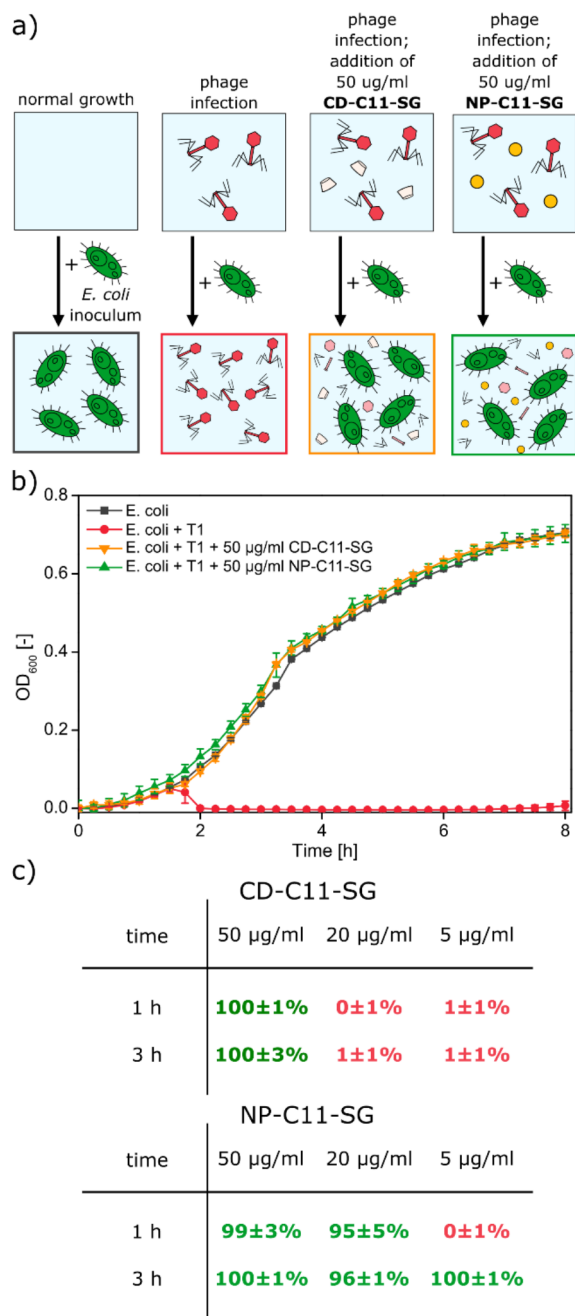

Figure 7. Protective effect of prepared antiphage compounds in the practical application of bacterial culture contaminated with T1 phages. (a) Four cases were investigated: normal culture of bacteria, bacterial growth contaminated with bacteriophages, bacterial culture contaminated with phages, and protected by 0.05 mg/mL of CD-C11-SG or 0.05 mg/mL of NP-C11-SG. (b) Bacterial growth monitored for all four cases by measurement of optical density at 600 nm (OD_{600}). (c) Protective effect investigated for various times of incubation and concentrations of antiphage compounds. Presented values are normalized OD_{600} after 8 h of bacterial culture growth.
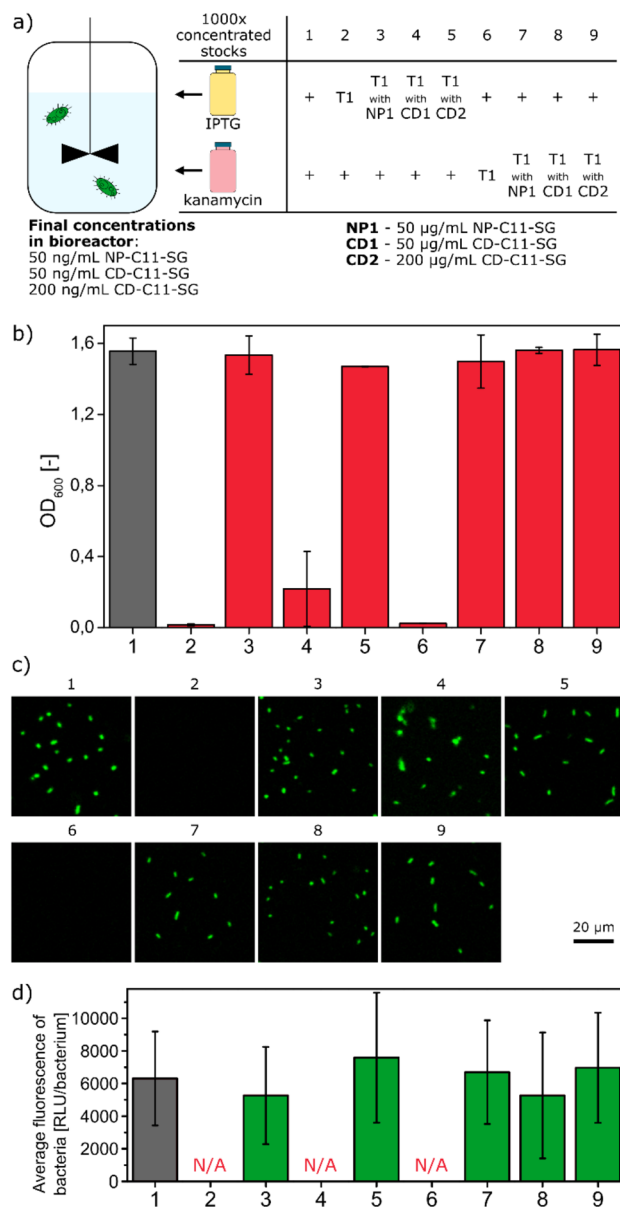
Figure 8. Protective effect of prepared antiphage compounds in the practical application of infection in stocks of antibiotic (kanamycin) or expression inducer (IPTG). (a) Nine samples of bacterial cultures *E. coli* BL21 DE3 (expressing GFP) prepared from various versions of kanamycin and IPTG stocks: noninfected ("+"), infected with phage T1 ("T1"), contaminated with T1 phages but protected with CD-C11-SG ("T1 with CD1", "T1 with CD2"), and contaminated with phages T1 but protected with NP-C11-SG ("T1 with NP1"). (b) Optical density after 24 h of growth of various bacterial culture samples. (c) Confocal microscopy after 24 h growth of various samples of bacterial cultures *E. coli* BL21 DE3. The fluorescence of bacteria confirms that the addition of CD-C11-SG and NP-C11-SG did not disturb the expression of GFP protein. (d) Statistical analysis of fluorescence intensity of bacteria in various samples. More than 550 bacteria were analyzed for each sample. Samples 2, 4, and 6 did not have enough bacteria for significant statistical analysis.

fected with T1 phages. To some of them, we added NP-C11-SG or CD-C11-SG. After 3 h of incubation of the stocks at 37 °C, we used them to prepare a bacterial culture of *E. coli* BL21 DE3 genetically modified to produce green fluorescent protein (GFP). In total we prepared nine different samples of growing liquid bacteria cultures, containing various variants of prepared

stocks), the bacteriophages killed all the bacteria. The addition of antiphage compounds prevented phage infection (samples 3–5 and 7–9). In almost every case, using 50 μg/mL antiphage compounds was enough for a fully protective effect. Only in the case of CD-C11-SG in the IPTG stock was 200 μg/mL cyclodextrins required to effectively deactivate bacteriophages.

As a next step, we evaluated if the addition of antiphage compounds influenced the bacterial expression of the proteins. For that purpose, we evaluated bacteria grown in all samples with confocal microscopy. As presented in Figure 8c,d, in all cases bacteria have similar florescent intensity, which proves that GFP was expressed and our compounds are not inhibiting bacterial expression systems.

It is also important to mention, that stocks of kanamycin and IPTG were 1000× concentrated; thus, they were added to the culture medium in a 1:1000 ratio. As a result, the initial concentration of 50–200 μg/mL of our antiphage compound in stocks was reduced by 3 orders of magnitude to 50–200 ng/mL in the bioreactor. Thus, the final concentrations in the bioreactor are 7.1 nM CD-C11-SG and only 75 pM NP-C11-SG. As a result, in such cases only very small amounts of our active compounds are needed. For example, a midscale bioreactor of a volume of 1 m^3 requires only 1 L of 1000× concentrated stocks of antibiotics and ITPG. Thus, only 50 mg of nanoparticles or 200 mg of cyclodextrins would be needed per single bioreactor run.

CONCLUSIONS

We believe that the presented approach is an important step toward designing safe, cost-effective, and efficient solutions against phage infections in industrial bioreactors. Our antiphage compounds allow for irreversible deactivation of various types of T phages in just 1 h at 37 °C and are nontoxic for both bacteria and eukaryotic cells. We prepared compounds based on two different cores: gold nanoparticle or beta-cyclodextrin. In both cases, the core was modified with hydrophobic linkers composed of 11 aliphatic carbons and ended with peptide selective for bacteriophages.

We proved that selective virucidal antivirals can be utilized against nonenveloped and water-borne viruses and that peptides can be used as a selective element of such design. As little as 50 μg/mL was enough to create a protective effect. The presented technology not only allowed for the protection of bacteria directly inside the environment of the bioreactor but was also effective as a safe additive to stocks of antibiotics and expression inducers. This is especially important since those stocks cannot be autoclaved and thus are a common source of phage contamination.

MATERIALS AND METHODS

Phage Display. Briefly, phage display was done using phage libraries containing phages M13 with random 7- or 12-mer peptides fused to a minor coat protein (pIII) (Ph.D.-7 Phage Display Peptide, Ph.D.-12 Phage Display Peptide, New England Biolabs) against phages T1 as a target. Target was immobilized on magnetic beads (Dynabeads M-280 Tosylactivated, Thermo Fisher). Three cycles of phage display were performed. After that, sequences of 25 randomly selected peptides were identified. A detailed explanation is provided in the Supporting Information.

Surface Plasmon Resonance. To study interactions between phages T1 and developed peptides, SPR analysis was used. We used the device Biacore 8K (Cytiva) and an S-Biacore chip. First, we prepared 10 μg/mL solutions of peptides "SG", "EG", "SR", and "AT"

in PBS buffer. Peptides were immobilized in separate channels of the chip. A 60 s cycle of immobilization resulted in 600–800 Relative Units (RU) of SPR signal. Then, we prepared a series dilution of T1 phages in buffer TM containing 0.005% of P20 surfactant (Cytiva). Surfactant was added to avoid nonspecific interaction between phages and streptavidin on the chip surface. Prepared concentrations of phages were 5×10^{10}, 1×10^{10}, 2×10^{9}, 4×10^{8}, and 8×10^{7} pfu/mL. Solutions with phages were run one by one through channels with immobilized peptides (starting from the lowest concentration of phages), and the SPR signal was measured.

Synthesis of Compounds and Nanoparticles. The starting materials were purchased from Sigma-Aldrich if not otherwise stated. Heptakis-(6-bromo-6-deoxy)-beta-cyclodextrin (CD-Br) was purchased from Cyclodextrin-Shop, Netherlands. Peptides were purchased from GL Biochem, China. 11-Amino-1-undecanethiol and 2-(2-(2-(2-aminoethoxy)ethoxy)ethoxy)ethanethiol (HS-EG4-NH2) were purchased from Prochimia Surfaces, Poland. Care was taken to use a freshly synthesized batch to minimize the presence of disulfides.

Synthesis of Oleylamine-Coated Nanoparticles (NP-oleylamine). First, gold salt (HAuCl$_4$·3H$_2$O; 1 mmol) was dissolved in 32 mL of oleylamine and 40 mL of n-octane. The solution was put under argon atmosphere. Then, t-butylamine-borane complex (t-BuNH$_2$BH$_3$; 2 mmol) dissolved in 8 mL of oleylamine was added via one-shot addition (using a syringe) to the mixed solution of gold salt. The reaction was continued for an additional 2 h at room temperature (RT), and then 60 mL of ethanol was added to the solution. Nanoparticles precipitated in ethanol were then washed by centrifugation using ethanol. Residual ethanol was dried in the open air.

Synthesis of Amine-Coated Nanoparticles (NP-C11-NH2). First, 50 mg of oleylamine-coated nanoparticles (NP-oleylamine) were dissolved in 30 mL of dichloromethane (DCM). Next, 28.6 mg of 11-amino-1-undecanethiol ligand was dissolved in 30 mL of 1 mM HCl aqueous solution (pH 3). Both solutions were stirred together for 2 days at RT. During that time, nanoparticles were transferred from DCM to the aqueous phase, indicating the end of successful ligand exchange. Then, the aqueous phase with nanoparticles was collected and water was removed by freeze-drying. Dry nanoparticles were redispersed in 40 mL of ethanol and washed by centrifugation using ethanol. Finally, nanoparticles were purified on Amicon Ultra-15 centrifugal filter devices (10k or 30k NMWL) first with 100 μM HCl (pH 3) and then with Milli-Q water. The particles were then suspended in a small amount of water (~2 mL) and freeze-dried.

Synthesis of Amine-Coated Nanoparticles with Hydrophilic Linker (NP-EG4-NH2). The synthesis was similar to the that of NP-C11-NH2 nanoparticles. The only difference was that 52 mg of HS-EG4-NH2 dissolved in 30 mL of Milli-Q water was used as ligand solution.

Synthesis of Peptide-Coated Nanoparticles (NP-C11-SG, NP-C11-HS, NP-C11-PH, and NP-EG4-SG). First, 15 mg of amine-coated nanoparticles (NP-C11-NH2), 22.6 mg of peptide SG, 7.0 mg of 1-ethyl-3-(3-(dimethylamino)propyl)carbodiimide (EDC), and 4.2 mg of N-hydroxysuccinimide (NHS) were dissolved in 1.5 mL of dimethyl sulfoxide (DMSO). To synthesize nanoparticles NP-C11-HS and NP-C11-PH, we used peptides HS and PH, respectively. To synthesize nanoparticles NP-EG4-SG, we used nanoparticles NP-EG4-NH2. The solution of peptides, nanoparticles, EDC, and NHS was mixed for 24 h at RT. Next, 70 mL of Milli-Q was added, and nanoparticles were purified with Milli-Q water on Amicon Ultra-15 centrifugal filter devices (30k NMWL). The particles were then suspended in a small amount of water (~2 mL) and freeze-dried.

Synthesis of Amine-Covered Cyclodextrins (CD-C11-NH2). First, 100 mg of 11-amino-1-undecanethiol ligand and 62.7 mg of CD-Br was dissolved in 1 mL of dimethylformamide (DMF). Then, 85 mg of triethylamine dissolved in 1.5 mL of DMF was added to the mixture, and the solution was stirred for 4 days at 60 °C. DMF was removed under reduced pressure, and the powder was redissolved in chloroform, which was then also removed under reduced pressure. The DMF-free powder was then dissolved in a 1:1 mixture of

chloroform and DMSO and dialyzed in an RC dialysis membrane (1 kDa NMWL). After 3 days of dialysis, the solvent was removed under reduced pressure.

Synthesis of Amine-Covered Cyclodextrins with Hydrophilic Linker (CD-EG4-NH2). First, 130 mg of HS-EG4-NH2 ligand was dried under vacuum to remove residual water. Then, the dried ligand was dissolved with 54.3 mg of CD-Br in 1 mL of dry DMF. Next, 97.9 mg of triethylamine dissolved in 1 mL of dry DMF was added to the mixture, and the solution was mixed under an argon atmosphere for 4 days at 60 °C. DMF was removed under reduced pressure, and the powder was redissolved in chloroform, which was then also removed under reduced pressure. The dried powder was dissolved in 2 mL of DMSO and dialyzed in an RC dialysis membrane (1 kDa NMWL). After 4 days of dialysis, the sample was freeze-dried.

Synthesis of Peptide-Covered Cyclodextrins (CD-C11-SG, CD-C11-HS, CD-C11-PH, and CD-EG4-SG). First, 15 mg of amine-covered cyclodextrins (CD-C11-NH2), 60.5 mg of peptide SG, 37.3 mg of EDC and 22.4 mg of NHS were dissolved in 1.5 mL of DMSO. To synthesize cyclodextrins CD-C11-HS and CD-C11-PH, we used peptides "HS" and "PH", respectively. To synthesize cyclodextrin CD-EG4-SG, we used cyclodextrin CD-EG4-NH2. The solution of peptides, cyclodextrin, EDC, and NHS was mixed for 24 h at RT. Then, the mixture was dialyzed in RC dialysis membrane (2 kDa NMWL) in DMSO and then in water. Finally, cyclodextrins were freeze-dried.

Characterization of Compounds and Nanoparticles. The size distribution of NPs was calculated based on TEM analysis. A drop of NPs (4 μL; 0.1−0.5 mg/mL) was deposited onto a 400-mesh carbon-supported copper grid and left to dry. All TEM images were acquired using an FEI TALOS electron microscope with an acceleration voltage of 200 kV equipped with a Ceta CCD camera. Images of the NPs were analyzed using Fiji software, and their diameters were calculated using a homemade script compatible with this software.

To analyze the purity of prepared cyclodextrins, HPLC qualitative analyses were conducted on a 1260 Infinity II HPLC system (Agilent Technologies). 90 μL aliquots of cyclodextrins were injected onto a 9.4 × 250 mm^2, 5 μm, Agilent Zorbax 300SB-C18 column heated at 45 °C. A binary gradient system consisted of A (water with 0.01% formic acid) and B (acetonitrile with 0.01% formic acid). Sample separation was carried out at 3 mL/min over a 20 min total run time. The initial condition was 70/30 v/v A/B. The proportion of the solvent B was linearly increased to 45/55 v/v A/B, from 0 to 15 minutes. From 15 to 16 minutes the percentage of B was further linearly increased to 40/60 v/v A/B, and left constant until min 26. A final increase to 30/70 v/v A/B was applied to wash the column for 15 min more, followed by an additional 15 min of column re-equilibration to initial conditions. The same method was applied to blank injections to ensure that no carryover was interfering with the measurements (data not shown). Detection was operated in the 1260 Infinity II HPLC DAD. The data showed consists of the extracted chromatogram at 254 nm with a bandwidth of 4 nm.

^{1}H NMR analysis was performed to control the purity and quality of prepared nanoparticles and cyclodextrins. In the case of nanoparticles, the absence of sharp peaks in the NMR spectrum obtained for the solution of nanoparticles suspended in water indicated a lack of impurities, such as free unbound ligands. The chemical composition of the ligand covering the nanoparticles was assessed by the ^{1}H NMR analysis after etching the nanoparticles with iodine. The etching solution was iodine (20 mg) dissolved in methanol-d_4 (1 mL). Etching was obtained by suspending NPs (5 mg) in the etching solution (0.6 mL) for 30 min under sonication.

To evaluate the number of peptides attached to nanoparticles and cyclodextrins, we performed elemental analysis. XPS measurements were carried out using a PHI VersaProbe II scanning XPS microprobe (Physical Instruments AG, Germany). Analysis was performed using a monochromatic Al Kα X-ray source of 24.8 W power with a beam size of 100 μm. The spherical capacitor analyzer was set at a 45° takeoff angle with respect to the sample surface. The pass energy was 46.95 eV yielding a full width at half-maximum of 0.91 eV for the Ag 3d$_{5/2}$ peak. Curve fitting was performed using the PHI Multipak software.

Dose−Response Assay. Approximately 5 × 10^3 pfu/mL phages were incubated in sterile tap water with various concentrations of nanoparticles or cyclodextrins at 37 °C for 3 h. As a control, samples with phages without any antiphage compounds were used. The number of phages was measured via the plaque count method. In this approach, the bottom LB-agar medium (20 mL) was poured onto a plastic Petri dish and left to solidify. Then, the top LB-agar, i.e., LB medium with 0.5% agar (4 mL), was mixed with an overnight culture of *E. coli* BL21 (200 μL) and poured onto the plate. Droplets of each sample (5 μL) were spotted on the top agar layer. Plaques were counted after the incubation of the plates at 37 °C for 24 h. All experiments were performed in duplicates.

Virucidal Assay. Phages (∼5 × 10^6 pfu/mL) were incubated in sterile tap water with 200 μg/mL nanoparticles or cyclodextrins at 37 °C for 3 h. The number of active phages was then measured by the plaque count method. In this approach, the bottom LB-agar medium (20 mL) was poured onto a plastic Petri dish and left to solidify. Then, the top LB-agar, i.e., LB medium with 0.5% agar (4 mL), was mixed with an overnight culture of *E. coli* BL21 (200 μL) and poured onto the plate. Dilutions of phage solution (10-fold) were prepared, and droplets of each dilution (5 μL) were spotted on the top agar layer. Plaques were counted after the incubation of the plates at 37 °C for 24 h. All experiments were performed in duplicates.

Antibacterial Assay. Overnight culture of bacteria *E. coli* BL21 was diluted 200x in LB medium containing various concentrations of nanoparticles or cyclodextrins. Then, the growth of the bacterial culture was observed by optical density (OD$_{600}$) measurement. To calculate dose response, the optical density after 6 h of incubation was compared. All experiments were performed in triplicates.

Cytotoxicity Test. The toxicity of NPs was examined using MTS [3-(4,5-dimethylthiazol-2-yl)-5-(3-carboxymethoxyphenyl)-2-(4-sulfophenyl)-2H-tetrazolium] assay. Vero cell cultures (African green monkey fibroblastoid kidney cells ATCC CCL-81) seeded in 96-well plates were incubated in DMEM (Gibco-BRL, Gaithersburg, MD) supplemented with 2% FBS with different concentrations of nanoparticles or cyclodextrins for 24 h. Cell viability was determined using the CellTiter 96 Proliferation Assay Kit (Promega, Madison, WI) according to the manufacturer's instructions. Absorbance was measured using a Microplate Reader (Model 680, BIORAD) at 490 nm. Cells incubated without nanoparticles nor cyclodextrins were used as the negative control. The effect on cell viability at different concentrations of nanoparticles or cyclodextrins was expressed as a percentage of live cells, by comparing the absorbance of treated cells with those of the cells incubated with the culture medium. All experiments were performed in triplicates.

Real Application Test of Infected Bacteria-Based Bioreactor. First, T1 bacteriophages (500 pfu/mL) were incubated with NP-C11-SG nanoparticles or CD-C11-SG cyclodextrins (50, 20, or 5 μg/mL) at 37 °C for 1 or 3 h. Then, to these solutions was added an inoculum of bacteria *E. coli* BL21 in LB medium. As controls, samples containing only bacteria (normal bacterial growth) and bacteria with T1 bacteriophages were prepared. The growth of bacteria was controlled by measuring the optical density (OD$_{600}$), which can be directly correlated with the number of bacteria in the solution. All experiments were performed in five repetitions.

Real Application Test of Infected Stocks of Kanamycin and IPTG. Aqueous stocks of 50 mg/mL kanamycin and 1 M IPTG were infected with 4 × 10^3 pfu/mL T1 phages. Then, 50 μg/mL NP-C11-SG, 50 μg/mL of CD-C11-SG, or 200 μg/mL CD-C11-SG was added to each solution. The stocks were then incubated at 37 °C for 3 h. Such prepared stocks were used to prepare the bacterial culture of *E. coli* BL21 DE3. The strain harbored plasmids coding GFP and providing resistance to chloramphenicol and kanamycin. LB (10 mL) was mixed with 10 μL of an overnight culture of *E. coli* BL21 DE3, 10 μL of 25 mg/mL chloramphenicol stock, 10 μL of 50 mg/mL kanamycin stock, and 10 μL of 1 mM IPTG stock. Chloramphenicol stock was not infected with phages, because it is an ethanol-based stock and phages cannot survive in it. After 24 h, the optical density at wavelength 600 nm was measured to evaluate bacterial growth. Confocal imaging was done using Inverted Leica DMi8 microscope

with Lumencor Sola SM II LED laser and LAS-X software. Image analysis was done in ImageJ software. All experiments were performed in duplicates.

ASSOCIATED CONTENT

ⓈⒾ Supporting Information

The Supporting Information is available free of charge at https://pubs.acs.org/doi/10.1021/acsnano.2c07896.

AUTHOR INFORMATION

Corresponding Authors

Łukasz Richter − Institute of Materials, Ecole Polytechnique Fédérale de Lausanne, 1015 Lausanne, Switzerland; Email: lukaszrichter@gmail.com

Francesco Stellacci − Institute of Materials, Ecole Polytechnique Fédérale de Lausanne, 1015 Lausanne, Switzerland; Institute of Bioengineering, Ecole Polytechnique Fédérale de Lausanne, 1015 Lausanne, Switzerland; Present Address: Global Health Institute, Ecole Polytechnique Fédérale de Lausanne, 1015 Lausanne, Switzerland; ⓞ orcid.org/0000-0003-4635-6080; Email: francesco.stellacci@epfl.ch

Authors

Corey Alfred Stevens − Institute of Materials, Ecole Polytechnique Fédérale de Lausanne, 1015 Lausanne, Switzerland

Paulo Jacob Silva − Institute of Materials, Ecole Polytechnique Fédérale de Lausanne, 1015 Lausanne, Switzerland

Laura Roset Julià − Institute of Materials, Ecole Polytechnique Fédérale de Lausanne, 1015 Lausanne, Switzerland; ⓞ orcid.org/0000-0003-4568-4242

Carla Malinverni − Institute of Materials, Ecole Polytechnique Fédérale de Lausanne, 1015 Lausanne, Switzerland

Lixia Wei − Institute of Materials, Ecole Polytechnique Fédérale de Lausanne, 1015 Lausanne, Switzerland

Marcin Łoś − Department of Molecular Genetics of Bacteria, Faculty of Biology, University of Gdańsk, 80-308 Gdańsk, Poland; Phage Consultants, 80-254 Gdańsk, Poland

Complete contact information is available at:
https://pubs.acs.org/10.1021/acsnano.2c07896

Notes

The authors declare no competing financial interest.

ACKNOWLEDGMENTS

REFERENCES

(1) Bogosian, G. Control of Bacteriophage in Commercial Microbiology and Fermentation Facilities. In *The Bacteriophages*; 2nd ed.; Oxford University Press: Oxford, 2006; pp 667−673.

(2) Whitman, W. B.; Coleman, D. C.; Wiebe, W. J. Prokaryotes: The Unseen Majority. *Proc. Natl. Acad. Sci. U. S. A.* **1998**, *95* (12), 6578−6583.

(3) Łoś, M. Contamination Concerns. *Eur. Biopharm. Rev.* **2010**, *51*, 78−80.

(4) Jończyk, E.; Kłak, M.; Międzybrodzki, R.; Górski, A. The Influence of External Factors on Bacteriophages-Review. *Folia Microbiol.* **2011**, *56* (3), 191−200.

(5) Los, M. Minimization and Prevention of Phage Infections in Bioprocesses. *Methods Mol. Biol.* **2012**, *834*, 305−315.

(6) Gilbert, G. L.; Gambill, V. M.; Spiner, D. R.; Hoffman, R. K.; Phillips, C. R. Effect of Moisture on Ethylene Oxide Sterilization. *Appl. Microbiol.* **1964**, *12* (6), 496−503.

(7) Bienek, C.; MacKay, L.; Scott, G.; Jones, A.; Lomas, R.; Kearney, J. N.; Galea, G. Development of a Bacteriophage Model System to Investigate Virus Inactivation Methods Used in the Treatment of Bone Allografts. *Cell Tissue Bank.* **2007**, *8* (2), 115−124.

(8) Atamer, Z.; Samtlebe, M.; Neve, H. J.; Heller, K. J.; Hinrichs, J. Review: Elimination of Bacteriophages in Whey and Whey Products. *Front. Microbiol.* **2013**, *4*, 00191.

(9) Guglielmotti, D. M.; Mercanti, D. J.; Reinheimer, J. A.; Quiberoni, A. del L. Review: Efficiency of Physical and Chemical Treatments on the Inactivation of Dairy Bacteriophages. *Front. Microbiol.* **2012**, *2*, 00282.

(10) Joe, Y. H.; Woo, K.; Hwang, J. Fabrication of an Anti-Viral Air Filter with SiO2-Ag Nanoparticles and Performance Evaluation in a Continuous Airflow Condition. *J. Hazard. Mater.* **2014**, *280*, 356−363.

(11) Bromberg, L.; Bromberg, D. J.; Hatton, T. A.; Bandín, I.; Concheiro, A.; Alvarez-Lorenzo, C. Antiviral Properties of Polymeric Aziridine- and Biguanide-Modified Core-Shell Magnetic Nanoparticles. *Langmuir* **2012**, *28* (9), 4548−4558.

(12) Matsushita, T.; Shirasaki, N.; Matsui, Y.; Ohno, K. Virus Inactivation during Coagulation with Aluminum Coagulants. *Chemosphere* **2011**, *85* (4), 571−576.

(13) Gilcrease, E.; Williams, R.; Goel, R. Evaluating the Effect of Silver Nanoparticles on Bacteriophage Lytic Infection Cycle-a Mechanistic Understanding. *Water Res.* **2020**, *181*, 115900.

(14) Gokulan, K.; Bekele, A.; Drake, K.; Khare, S. Responses of Intestinal Virome to Silver Nanoparticles: Safety Assessment by Classical Virology, Whole-Genome Sequencing and Bioinformatics Approaches. *Int. J. Nanomedicine* **2018**, *13*, 2857−2867.

(15) Shimabuku, Q. L.; Ueda-Nakamura, T.; Bergamasco, R.; Fagundes-Klen, M. R. Chick-Watson Kinetics of Virus Inactivation with Granular Activated Carbon Modified with Silver Nanoparticles and/or Copper Oxide. *Process Saf. Environ. Prot.* **2018**, *117*, 33−42.

(16) De Gusseme, B.; Sintubin, L.; Baert, L.; Thibo, E.; Hennebel, T.; Vermeulen, G.; Uyttendaele, M.; Verstraete, W.; Boon, N. Biogenic Silver for Disinfection of Water Contaminated with Viruses. *Appl. Environ. Microbiol.* **2010**, *76* (4), 1082−1087.

(17) Shimabuku, Q. L.; Arakawa, F. S.; Fernandes Silva, M.; Ferri Coldebella, P.; Ueda-Nakamura, T.; Fagundes-Klen, M. R.; Bergamasco, R. Water Treatment with Exceptional Virus Inactivation Using Activated Carbon Modified with Silver (Ag) and Copper Oxide (CuO) Nanoparticles. *Environ. Technol.* **2017**, *38* (16), 2058−2069.

(18) Cheng, R.; Kang, M.; Zhuang, S.; Wang, S.; Zheng, X.; Pan, X.; Shi, L.; Wang, J. Removal of Bacteriophage F2 in Water by Fe/Ni Nanoparticles: Optimization of Fe/Ni Ratio and Influencing Factors. *Sci. Total Environ.* **2019**, *649*, 995−1003.

(19) Mazurkow, J. M.; Yüzbasi, N. S.; Domagala, K. W.; Pfeiffer, S.; Kata, D.; Graule, T. Nano-Sized Copper (Oxide) on Alumina Granules for Water Filtration: Effect of Copper Oxidation State on

Virus Removal Performance. *Environ. Sci. Technol.* **2020**, *54* (2), 1214−1222.

(20) Syngouna, V. I.; Chrysikopoulos, C. V. Inactivation of MS2 Bacteriophage by Titanium Dioxide Nanoparticles in the Presence of Quartz Sand with and without Ambient Light. *J. Colloid Interface Sci.* **2017**, *497*, 117−125.

(21) Cho, M.; Cates, E. L.; Kim, J.-H. Inactivation and Surface Interactions of MS-2 Bacteriophage in a TiO2 Photoelectrocatalytic Reactor. *Water Res.* **2011**, *45* (5), 2104−2110.

(22) Ledeboer, A. M.; Bezemer, S.; de Haard, J. J. W.; Schaffers, I. M.; Verrips, C. T.; van Vliet, C.; Düsterhöft, E.-M.; Zoon, P.; Moineau, S.; Frenken, L. G. J. Preventing Phage Lysis of Lactococcus Lactis in Cheese Production Using A Neutralizing Heavy-Chain Antibody Fragment from Llama. *J. Dairy Sci.* **2002**, *85* (6), 1376−1382.

(23) Veesler, D.; Dreier, B.; Blangy, S.; Lichière, J.; Tremblay, D.; Moineau, S.; Spinelli, S.; Tegoni, M.; Plückthun, A.; Campanacci, V.; Cambillau, C. Crystal Structure and Function of a DARPin Neutralizing Inhibitor of Lactococcal Phage TP901−1. *J. Biol. Chem.* **2009**, *284* (44), 30718−30726.

(24) Ferreira, R. D. G.; Azzoni, A. R.; Freitas, S. Techno-Economic Analysis of the Industrial Production of a Low-Cost Enzyme Using E., Coli: The Case of Recombinant *β*-Glucosidase. *Biotechnol. Biofuels* **2018**, *11* (1), 81.

(25) Murata, A.; Kitagawa, K.; Saruno, R. Inactivation of Bacteriophages by Ascorbic Acid. *Agric. Biol. Chem.* **1971**, *35* (2), 294−296.

(26) Baltz, R. H. Bacteriophage-Resistant Industrial Fermentation Strains: From the Cradle to CRISPR/Cas9. *J. Ind. Microbiol. Biotechnol.* **2018**, *45* (11), 1003−1006.

(27) Richter, Ł.; Paszkowska, K.; Cendrowska, U.; Olgiati, F.; Silva, P. J.; Gasbarri, M.; Guven, Z. P.; Paczesny, J.; Stellacci, F. Broad-Spectrum Nanoparticles against Bacteriophage Infections. *Nanoscale* **2021**, *13* (44), 18684−18694.

(28) Kocabiyik, O.; Cagno, V.; Silva, P. J.; Zhu, Y.; Sedano, L.; Bhide, Y.; Mettier, J.; Medaglia, C.; Da Costa, B.; Constant, S.; Huang, S.; Kaiser, L.; Hinrichs, W. L. J.; Huckriede, A.; Le Goffic, R.; Tapparel, C.; Stellacci, F. Non-Toxic Virucidal Macromolecules Show High Efficacy Against Influenza Virus Ex Vivo and In Vivo. *Adv. Sci.* **2021**, *8* (3), 2001012.

(29) Cagno, V.; Andreozzi, P.; D'Alicarnasso, M.; Silva, P. J.; Mueller, M.; Galloux, M.; Goffic, R. Le; Jones, S. T.; Vallino, M.; Hodek, J.; Weber, J.; et al. Broad-Spectrum Non-Toxic Antiviral Nanoparticles with a Virucidal Inhibition Mechanism. *Nat. Mater.* **2018**, *17* (2), 195−203.

(30) Jones, S. T.; Cagno, V.; Janeček, M.; Ortiz, D.; Gasilova, N.; Piret, J.; Gasbarri, M.; Constant, D. A.; Han, Y.; Vuković, L. Modified Cyclodextrins as Broad-Spectrum Antivirals. *Sci. Adv.* **2020**, *6* (5), eaax9318.

(31) Rakhuba, D. V.; Kolomiets, E. I.; Szwajcer Dey, E.; Novik, G. I. Bacteriophage Receptors, Mechanisms of Phage Adsorption and Penetration into Host Cell. *Polish J. Microbiol.* **2010**, *59* (3), 145−155.

(32) Ong, Q.; Luo, Z.; Stellacci, F. Characterization of Ligand Shell for Mixed-Ligand Coated Gold Nanoparticles. *Acc. Chem. Res.* **2017**, *50* (8), 1911−1919.

(33) Yap, M. L.; Rossmann, M. G. Structure and Function of Bacteriophage T4. *Future Microbiol.* **2014**, *9* (12), 1319−1337.

(34) Roberts, M. D.; Martin, N. L.; Kropinski, A. M. The Genome and Proteome of Coliphage T1. *Virology* **2004**, *318* (1), 245−266.

(35) Balmert, S. C.; Zmolek, A. C.; Glowacki, A. J.; Knab, T. D.; Rothstein, S. N.; Wokpetah, J. M.; Fedorchak, M. V.; Little, S. R. Positive Charge of "Sticky" Peptides and Proteins Impedes Release from Negatively Charged PLGA Matrices. *J. Mater. Chem. B* **2015**, *3* (23), 4723−4734.

(36) Lerro, K. A.; Orlando, R.; Zhang, H. Z.; Usherwood, P. N. R.; Nakanishi, K. Separation of the Sticky Peptides from Membrane Proteins by High-Performance Liquid Chromatography in a Normal-Phase System. *Anal. Biochem.* **1993**, *215* (1), 38−44.